БЪЛГАРСКА АКАДЕМИЯ НА НАУКИТЕ • BULGARIAN ACADEMY OF SCIENCES

ГЕОХИМИЯ, МИНЕРАЛОГИЯ И ПЕТРОЛОГИЯ • 42 • СОФИЯ • 2005
GEOCHEMISTRY, MINERALOGY AND PETROLOGY • 42 • SOFIA • 2005

Oligocene pyroclastic rocks and a petrified forest in the Nanovitsa depression

Svetoslav Georgiev, Peter Marchev

Abstract. The 31Ma-old tuffs in the Nanovitsa depression of the Eastern Rhodopes preserve evidence of a series of large eruptions of acid pyroclastic rocks and one of the largest Oligocene natural disasters in the Rhodopes region. Intra-depression acid tuffs overlie Zvezdel, Dambalak and Sveti Ilia intermediate lava flows, as well pyroclastic rocks from the Borovitsa volcanic area (second acid volcanism) dated at 31.8 Ma. The pyroclastic sequence consists of two ignimbrite units (Raven and Sapdere type) and one mixed unit comprising air-fall tuffs and epiclastic rocks.

Air-fall deposits buried a forest, consisting of giant (up to 4 m in diameter) and smaller sub-vertical trees. The trees are silicified, with well-preserved wood structure. The presence of numerous sub-horizontal carbonized branches in the transitional level between the air-fall tuffs and the ignimbrites, as well as the well-developed radial cracks and gas-escape structures above the branches, suggest a quick deposition of both the air-fall tuffs and the ignimbrites from an eruption column. Careful examination of the orientation of the branches places constraints on the location of the vent that generated the eruption, which we argue to be to the NE of the Nanovitsa depression.

The ignimbrites are strongly zeolitized, which hinders the correct determination of their whole-rock chemical composition. Whole-rock analyses of a pumice clast and two melt inclusions in quartz phenocrysts show a high-K high-silica rhyolite composition for the magma. Compositional variations of plagioclase and biotite phenocrysts suggest a compositional zoning of the magma chamber. Pre-eruptive conditions of the rhyolite magma, calculated from phenocryst compositions using two-oxide thermometer and two-feldspar thermometers and barometer, ranged from 640 to 740°C and 2-3 kbar (~6.5-10 km).

Key words: pyroclastic rocks, petrified forest, Nanovitsa depression, Eastern Rhodopes
Addresses: S. Georgiev, P. Marchev - Geological Institute, Bulgarian Academy of Sciences, 1113 Sofia, Bulgaria; S. Georgiev, present address: Institute of Isotope Geology and Mineral Resources, ETH Zurich, Switzerland

Георгиев, С., П. Марчев. 2005. Олигоценски пирокластични скали и вкаменена гора в Нановишката депресия. *Геохим., минерал. и петрол.,* **42**, 47-65.

Резюме. Датираните на 31 Ма туфи в Нановишката депресия запазват доказателства за поредица големи ерупции на кисели пирокластични скали и една от големите природни катастрофи по времето на олигоцена на територията на Родопите. Киселите туфи на Нановишката депресия са разположени над средни по състав лавови потоци на вулканите Звездел, Дамбалък и Свети Илия, а така също и над датирани на 31.8 Ма пирокластични скали от Боровишката вулканска област (втори кисел вулканизъм). Пирокластичният разрез се състои от две игнимбритови единици (Равенски и Сапдеренски тип), и една съставна единица, включваща пеплопадни туфи и епикластични скали.

Пеплопадните отложения са затрупали гора, състояща се днес от гигантски (над 4 м диаметър) и по-малки, вертикално запазени дървесни стволове. Дърветата са силифицирани, с добре запазена дървесна структура. Присъствието на множество субхоризонтални овъглени клони в преходното ниво между пеплопадните туфи и игнимбритите, а така също и наличието на радиални следи от взривове и газово-сегрегационни структури над клоните, говорят за бързо отлагане на пеплопадните туфи и

игнимбритите от една ерупционна колона. Внимателното изследване на ориентировката на хоризонталните клони дава насоки за евентуалното положение на гърловата област на ерупцията, която според нас се е разполагала на североизток от Нановишката депресия.

Игнимбритите са силно зеолитизирани, което възпрепятства точното определяне на валовия химичен състав. Валови анализи на голям пемзов къс и микросондови анализи на две стъклени включения свидетелстват за високо калиев, високо силициев риолитов състав на магмата. Вариациите в състава на плагиоклазовите и биотитовите фенокристали в големи пемзови късове говорят за наличието на зонална по състав магмена камера. Предеруптивните условия на риолитовата магма, изчислени от съставите на съвместно съществуващи фенокристали по двуоксидния и двуфелдшпатовия термометър и барометър, варират от 640 до 740°C и 2-3 килобара (~6.5-10 km).

Introduction

During the Upper Eocene-Oligocene, the Eastern Rhodope zone in SE Bulgaria was the locus of extensive magmatic activity. The dominant type of volcanism was intermediate to silicic calc-alkaline to shoshonitic with subordinate basalts (Marchev et al., 1998, Yanev et al., 1998). Two major acid explosions deposited pyroclastic rocks over the entire Eastern Rhodopes. They are named first and second acid volcanism by Ivanov (1960) and recently precisely dated using the $^{40}Ar/^{39}Ar$ method by Singer and Marchev (2000), Marchev and Singer (2002), Moskovski et al. (2004). However, a number of areas in the Eastern Rhodopes occupied by large volumes of acid pyroclastic rocks remain weakly studied. One of these areas is the Nanovitsa depression, which seems to accommodate the latest eruptive activity in the Eastern Rhodopes (Goranov et al., 1995). Here we describe the geology of the area and provide petrological and $^{40}Ar/^{39}Ar$ data about pyroclastic rocks in this area. The depression provides an excellent opportunity for studies of different volcanic phenomena, including a world-class petrified forest.

Geological background and lithology of the studied area

The Nanovitsa depression is located between Paleogene polyphase volcanoes Zvezdel, Dambalak and Sveti Ilia in the Momchilgrad-Arda volcanic region of the Eastern Rhodopes volcanic area. It is filled with acid pyroclastic rocks, overlying a sedimentary formation (Fig. 1) but, untill now, only a few studies have dealt with the geology of the depression. As part of the large Eastern Rhodope Paleogene depression, the pyroclastic rocks of the Nanovitsa depression have been briefly characterized in the works of Goranov (1960), Ivanov (1961), Bahneva and Stefanov (1974), Boyanov and Goranov (2001). These authors describe the rocks as massive or coarse bedded rhyolitic tuffs formed during the final stages of the volcanic activity. Moskovski et al. (1990) provide the most detailed volcanological description of the Nanovitsa depression stratigraphy. Following the ideas of Ivanov (1960), Goranov et al. (1995) presented a stratigraphic subdivision of the pyroclastic rocks and ascribed them to the formation of the third acid volcanism ($10Pg_3$). The northern part of the Nanovitsa depression is considered by Georgiev et al. (2000) to be a separate volcano. Based on interpretation of geophysical data these authors argue that the Nanovitsa depression is a caldera structure.

The proposed subdivision of the rocks in this paper is based mainly on the lithology and the mode of formation of the different rocks. The following units can be distinguished: a sedimentary formation; a pyroclastic formation that comprises Tatul rhyolitic tuffs, Sapdere ignimbrites, Raven ignimbrites; and a formation of organogenic limestones (Fig. 1).

The sedimentary formation is composed of stratified marls, sandstones and organogenic limestones, and sedimentary-volcanogenic rocks, which crop out in the lowermost parts of the depression. In the southern part, the

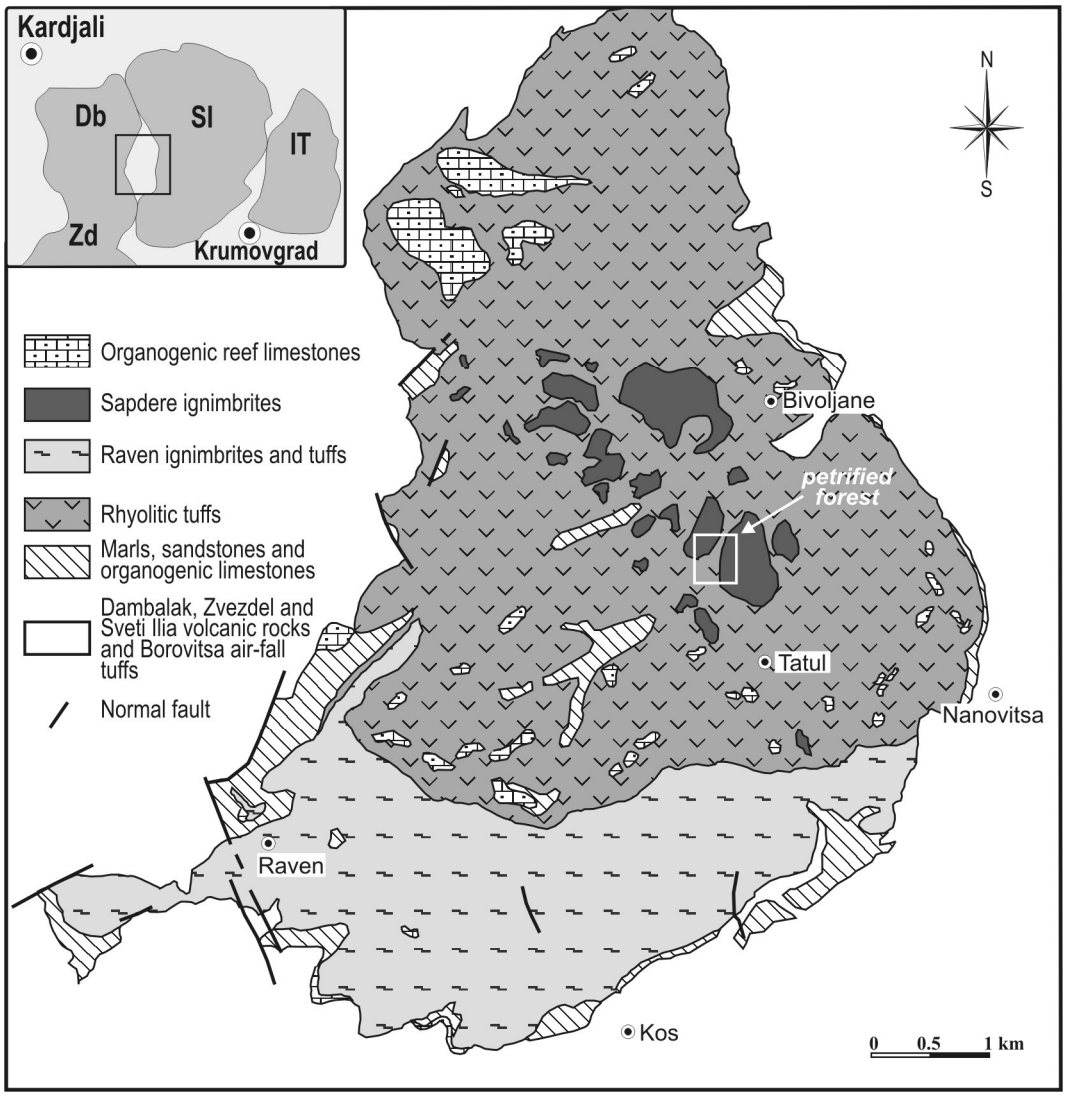

Fig. 1. Simplified geologic map of the Nanovitsa depression, showing the location of the petrified forest (modified after Moskovski et al., 1990). Inset – position of the Nanovitsa depression with respect to the surrounding volcanoes

Фиг. 1. Схематична геоложка карта на Нановишката депресия, показваща местоположението на "вкаменената гора" (по Moskovski et al., 1990, с изменения). Врезка – позиция на Нановишката депресия по отношение на околните вулкански постройки

sedimentary rocks normally overlie the last brecciated basaltic andesite lava flow of the Zvezdel volcano, whereas in the northern part, the pyroclastic rocks of the Nanovitsa depression overlie air-fall deposits of the second acid volcanism.

The sedimentary sequence comprises mostly finely stratified gray marls interbedded with layers of fine-grained sandstones and organogenic limestones. The sandstones contain a volcanoclastic component of andesitic composition. The stratification is subhorizontal or dips gently north (10-20°). Some localities in the southern part of the depression are characterized by cross stratification. The maximum thickness of the marls, sandstones and organogenic limestones formation can be observed near the village of Kos, where it is up to 60 m thick.

The pyroclastic formation comprises three units: the Tatul rhyolitic tuffs, the Sapdere ignimbrites and the Raven ignimbrites.

The Tatul rhyolitic tuffs, overlying the sedimentary rocks, are white to gray or pale yellow bedded or non-bedded rocks. In the western part of the depression, the contact between the Tatul tuffs and the sedimentary rocks is not sharp: there is a 10-25 m thick zone of lithological transition between the two formations. In the transitional zone, the amount and thickness of the marl layers decrease upwards at the expense of the tuff layers. In some localities (e.g. near the village of Kos) the rhyolitic tuffs overlie an uneven surface, washed out in the marls. Along the western border of Nanovitsa depression, the rhyolitic tuffs overlie the hornblende-biotite-two pyroxene andesites of the Dambalak volcano. The thickness of the rhyolitic tuffs varies from 10-20 to 120-150 m.

The rhyolitic tuffs are composed predominantly of juvenile material (pumice and glass shards) and subordinate lithic fragments (sediments, andesitic lavas), comprising less than 20 vol.% of the rock. In the lower parts of some sections, the rhyolitic tuffs contain numerous elongated lithic fragments of limestones and marls with well developed thermal haloes. The lithic fragments are imbricated, showing a direction of transport from west to east. According to the nongenetic, lithologic classification of pyroclastic fragments and aggregates (Fisher, 1961), the rhyolitic tuffs can be classified as lappili and ash tuffs. The uppermost levels of the rhyolitic tuffs contain pieces of silicified wood with maximum size of 30-50 cm. The so-called "petrified forest", described by Harkovska et al. (1992), is situated in the upper levels of the rhyolitic tuffs, northwest from the village of Tatul.

In the central and northeastern part of the depression, the rhyolitic tuffs are overlain by pyroclastic flow deposits named the Sapdere ignimbrites which crop out as distinct patches around 20×10 m, 20×50 m to 0.5 km^2 in size between the villages of Tatul and Bivoljane. The ignimbrites are deposited from at least four consecutive pyroclastic flows with a total thickness of several meters, and can be up to 60-70 m. Each pyroclastic flow was preceded by an air-fall and/or pyroclastic surge activity, which deposited the stratified tuffs that separate the ignimbrite units (Fig. 2). The alternation of ignimbrites and stratified air-fall deposits reflects major changes in the eruption column behaviour, which probably resulted from periodical narrowing of the vent.

The rocks are composed of bomb- to lapilli-sized pumice fragments and subordinate angular lithic fragments (rhyolites and rarely andesites) embedded in a matrix of vitric, crystal, and lithic ash (Harkovska et al., 1992). Generally, there is no sorting of the pyroclastic material. A reverse grading of the pumice clasts can be observed at some localities. The vitric fragments are glass shards, derived from the pulverization of pumice during eruption and emplacement. The most abundant phenocrysts in the pumice clasts are sanidine, quartz and plagioclase; biotite is in subordinate quantity. Magnetite and zircon also occur. The matrix of the ignimbrites contains similar crystals but the crystal content is higher compared to the crystal concentration in the pumice clasts. Such crystal enrichment can be explained by the winnowing out of vitric ash from the pyroclastic flow during its movement.

Fig. 2. View toward the north in the Sapdere canyon. Outcrop of the stratified rhyolitic tuffs and the four units of Sapdere ignimbrites. The vertical columns in the rhyolitic tuffs are silicified trees
Фиг. 2. Изглед на север в каньона на Сапдере. Разкритие на слоисти риолитови туфи и четирите единици на Сапдеренските игнимбрити. Вертикалните колони в риолитовите туфи представляват вкаменени дървета

This process, known as elutriation, effectively concentrates the denser crystal fragments into the main body of the flow, relative to the glass shards.

The southern part of the Nanovitsa depression is filled mostly with pyroclastic flow deposits named Raven ignimbrites. The Raven ignimbrites overlie the formation of marls, sandstones and organogenic limestones, the rhyolitic tuffs and, in the southwestern parts, some basaltic andesite and basalt lava flows of the Zvezdel volcano. The morphology and macroscopic features of the Raven ignimbrites are similar to those of the Sapdere ignimbrites: they are massive, partially welded devitrified pyroclastic rocks. The main differences are the abundance, composition and size of the lithoclasts.

The Raven ignimbrites contain lithoclasts of rhyolites (massive, brecciated, and layered), rhyolitic tuffs, silicified organogenic limestones, marls, sandstones, andesites, gneisses and perlitic clasts. The abundance and size of the lithoclasts decreases eastwards. In the western part of the studied area there can be observed soft-sediment deformation structures in the marls and sandstones beneath the contact of the ignimbrites and the sediments.

The central and northwestern parts of the depression are occupied by several bodies of organogenic reef limestones, overlying the rhyolitic tuffs. The size of the reef bodies varies from 10 × 20 m to 0.2 km^2 and their thickness is up to 20-30 m. They probably represent relicts from two big limestone plates. The reef limestones characterize the Paleogene

basin as of a shallow marine type - warm and with normal salinity (Boyanov et al., 2001).

Genetic interpretation and volcanological significance of the petrified forest

The lowermost part of Tatul rhyolitic tuffs has a submarine air-fall origin. The main part of the sequence, however, is of controversial origin. These tuffs have been considered to be deposited by a pyroclastic flow in a shallow marine environment. Other ideas include pyroclastic air-fall origin or an epiclastic origin (Moskovski et al., 1990), whereas Harkovska and Djourova (1994) provide evidences for a slump re-deposition origin for the middle part of the sequence. According to them, the rocks were formed by gravitational slumping of rhyolitic tuffs from the subaqueous and subareal slope of the Dambalak volcano. This hypothesis is consistent with the observed imbrication of lithic clasts in the rhyolitic tuffs. In places, the middle levels of the Tatul rhyolitic tuffs possess characteristics of ash-flow tuffs, deposited by a submarine pyroclastic flow. They are massive, with occasional vague bedding. In the massive levels, segregation structures can be observed. The presence of flattened glass shards, pumice clasts and thermal haloes around the marl lithoclasts indicates a high-temperature emplacement.

In the central part of the depression, the uppermost levels of the Tatul tuffs, just beneath the contact with the overlying Sapdere ignimbrites, are finely stratified and host numerous silicified trees and tree remnants, which form the spectacular and very informative volcanic phenomenon “petrified forest”.

The petrified forest comprises more than 20 upright trees and negative imprints from trees discovered in the deep valley of Sapdere river. The tree remnants are trunks ranging from 0.4 to 2 m in diameter and from 0.5 to 3.5 m in height (Fig. 3a, b). Three of the trunks have diameters over 3 m with the biggest one over 4 m (Fig. 3c, d). Apart from being an impressive natural phenomenon, the petrified forest is an unique site for volcanological studies. There are a number of studied and described petrified tree remnants and trees in pyroclastic rocks (Creber, Ash, 2004). However, most of the trees in these petrified forests are not preserved in an upright position. In cases where they are preserved upright, good exposures of the host pyroclastic rock are usually lacking.

Unlike other world examples, the petrified forest near Tatul comprises silicified and carbonized vertical and subvertical trees and tree remnants of impressive size, hosted in beautifully exposed pyroclastic rocks. From a volcanological point of view, this petrified forest can be described as a snap-shot of a spectacular volcanic phenomenon - generation, development and subsequent collapse of an eruption column.

The trees are completely silicified, with impressive retention of the wood structure. Some of the trees have well preserved bark and growth rings (Fig. 4a). The silicification has indurated and strengthened the trees and as a result of that they are more resistant to erosion than their host rocks.

The upright position of the trees, combined with the good stratification of the rhyolitic tuffs and the lack of evidences for high-temperature emplacement of the pyroclastic material (carbonization of the trees or welding) suggests that the rhyolitic tuffs have a subareal air-fall origin. Probably they were formed by precipitation of pyroclastic material from a high eruption column. The

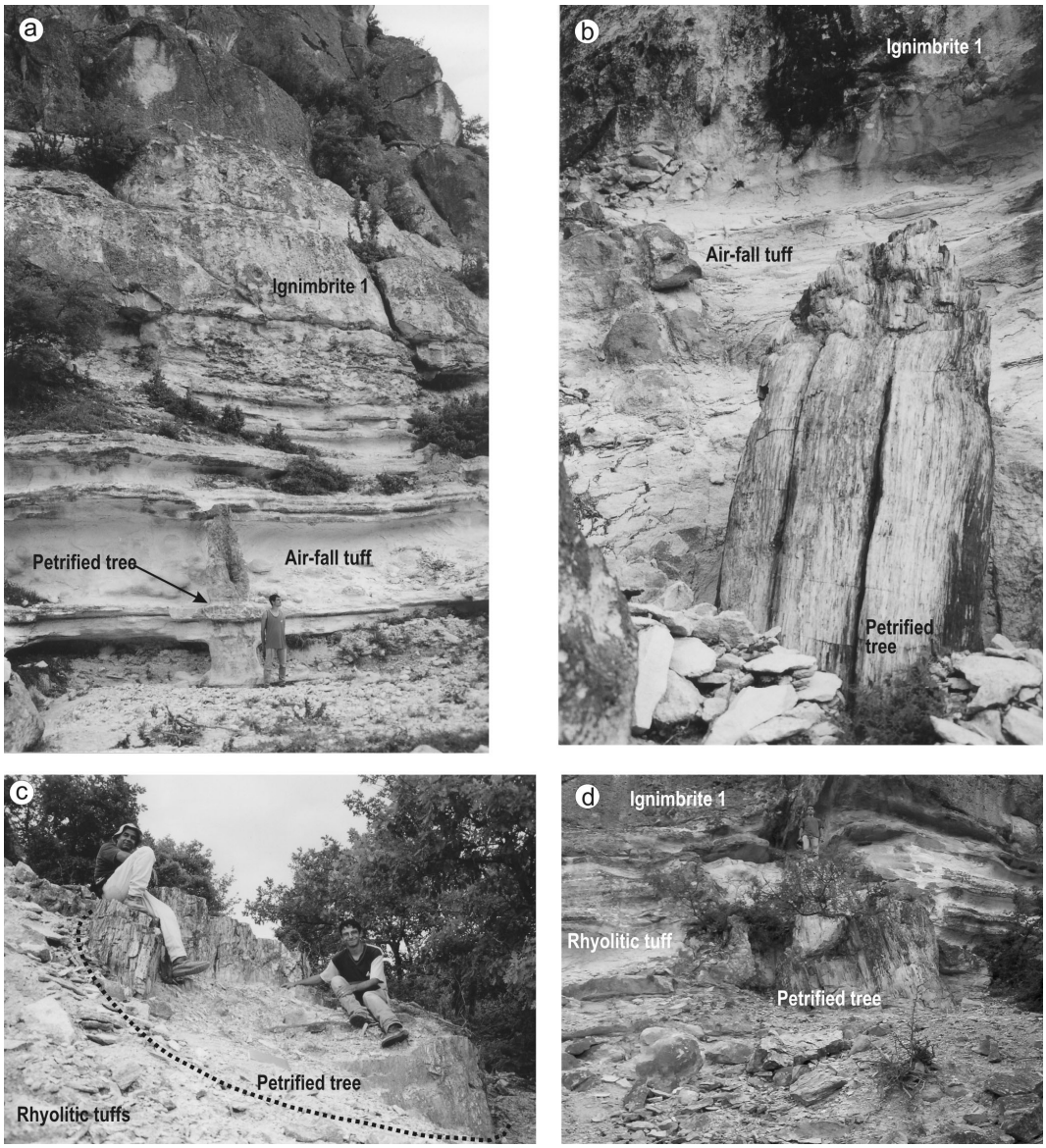

Fig. 3. Photographs showing: a) outcrop of the contact between the upper part of the rhyolitic tuffs with silicified trees and the lowermost pyroclastic flow (Sapdere ignimbrite); b) a partly preserved petrified tree; c) the biggest tree with diameter ~ 4 m; d) a young tree (~ 4 m) growing on the 31 Ma silicified tree

Фиг. 3. Снимки, показващи: а) разкритие на контакта между горната част на риолитов туф с вкаменено дърво и най-долния пирокластичен поток (Сапдеренски игнимбрит); b) частично запазено вкаменено дърво; c) най-голямото вкаменено дърво с диаметър ~ 4 м; d) младо дърво, прорастнало във силифицирано 31 млн. годишно дърво

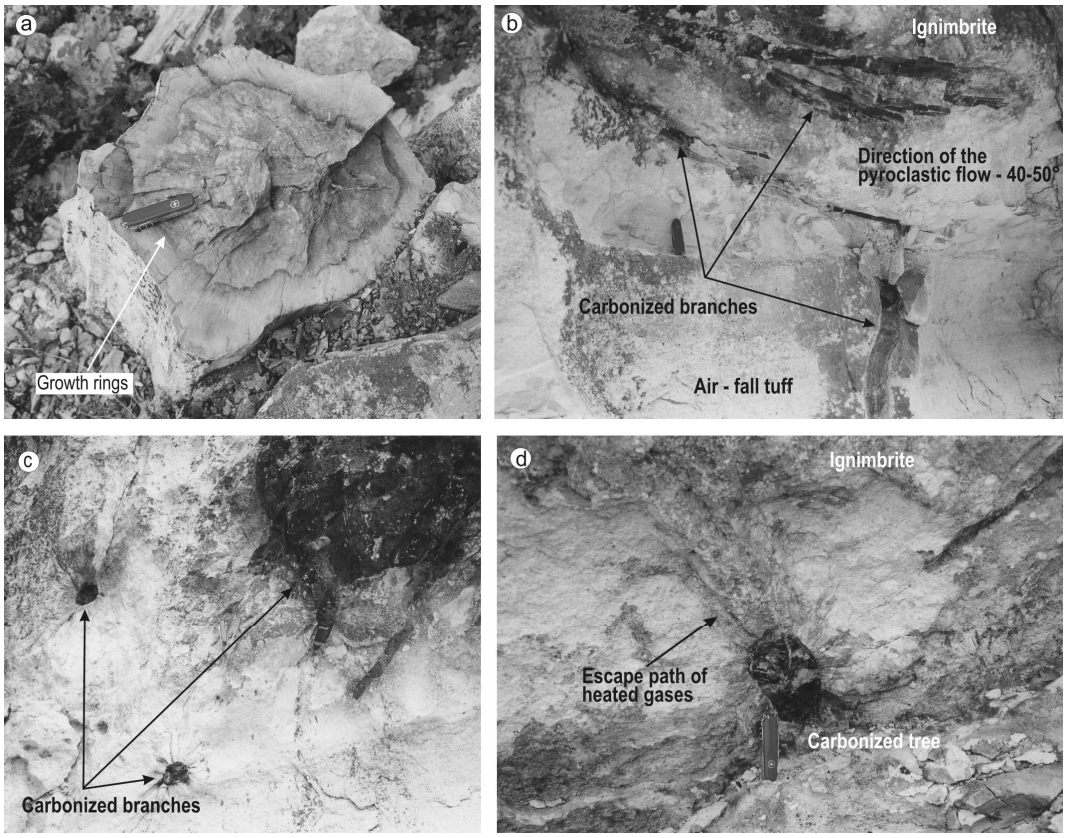

Fig. 4. Photographs showing: a) a silicified tree with perfectly preserved wood structure; b) an interface between air-fall tuff and the lowermost pyroclastic flow (Sapdere ignimbrite). The pyroclastic flow moved from right to left; c) radial cracks around branches; d) gas-escape structures above a carbonized branch
Фиг.4. Снимки, показващи: a) вкаменено дърво със добре запазена дървесна структура; b) граница между пеплопаден туф и най-долният пирокластичен поток (Сапдеренски игнимбрит). Посоката на придвижване на пирокластичния поток е отдясно наляво; c) радиални пукнатини около овъглени клонки; d) следи от отделените нагрети газове над овъглен клон

falling pyroclastic material was cooled by the air and simply buried the trees.

Eruption of the first pyroclastic flow is marked by numerous findings of carbonized sub-horizontal branches in the uppermost levels of the rhyolitic tuffs and the lowermost part of Sapdere ignimbrites (Fig. 4b). The carbonization of these branches can be interpreted as evidence for the high temperature of the pyroclastic material. The abundance of well-developed radial cracks (Fig. 4c) around the branches, preserved in cross-sections, strongly supports the hot emplacement of the ignimbrites. The cracks formed as the hot material heated and vaporized the water in the wood and the increased pressure resulted in bursts around the branches and fracturing of the dense pyroclastic material. There are also typical gas-escape structures above the charred trunks and branches in the ignimbrite (Fig. 4d). Their mode of formation is similar to those commonly found in ignimbrites gas-pipes (Cas, Wright, 1988; Francis, 1993), but here the source of the heated gasses is the wood material.

The presence of carbonized branches in the ignimbrite above the silicified trees indicates the genetic relationship between the air-fall deposit and the ignimbrite. The trees, buried by the volcanic ash were still alive when the pyroclastic flow passed, since the radial cracks suggest that the trees contained considerable amounts of water. The most probable explanation for the rapid emplacement of the flow is a collapse of the eruption column, which generated the air-fall deposit.

The location of the vent that produced the eruption can be inferred by close examination of a very thin branch at the contact of the rhyolitic tuffs and the ignimbrites (Fig. 4a). Unlike the other trunks and branches, that small carbonized branch was not crushed by the dense, hot and rapid pyroclastic flow. The branch was bent by the moving flow in a southwest direction, thus indicating a vent location to the northeast. This conclusion is confirmed by the general orientation of the numerous carbonized branches in a general NE-SW direction (45-60°).

Petrology and geochemistry of the ignimbrites

Analytical methods

Laboratory studies involved electron microprobe analyses (EMPA), X-ray diffraction, XRF and ICP-MS analyses, and $^{40}Ar/^{39}Ar$ age dating.

Microprobe data were collected from polished thin sections using a JEOL Superprobe 870 at the University of Florence (CNR, Centro di studi per la Minerogenesi e Geochimica Applicata), Italy. Operating conditions were typically a beam current of 10 nA and an accelerating voltage of 15 kV. Data were corrected following the method of Bence and Albee (1968). To minimize volatilization of the glass, the electron beam was rastered over an area ranging from 5 to 15 μm in diameter.

Major and trace element analyses of 5 samples were determined by XRF analysis. All samples except Zd97-1, which was analyzed at the University of Florence, have been analysed at the University of Lausanne. The trace element composition (except V, Cr, Co, Ni, Zn, Cu) of the sample Zd97-1 was determined by ICP/MS at the Washington State University (Pullman).

X-ray diffraction samples were analyzed on an automatic X-ray diffraction system D 500 Siemens at the Geological Institute of the Bulgarian Academy of Sciences.

$^{40}Ar/^{39}Ar$ experiments on sanidine from sample Zd97-1 were conducted using a CO_2 laser probe. Irradiation of the sample was completed at Oregon State University for 12 or 50 hours along with a 27.92 Ma sanidine from the Taylor Creek rhyolite (Duffield, Dalrymple, 1990) as the neutron fluence monitor. Isotopic measurement was made of the gas extracted by fusion of 6 grains using a defocused CO_2 laser beam. The isotopic composition of the gas was measured using an MAP 216 spectrometer at the University of Geneva, Switzerland.

Petrography

Several large pumice clasts were chosen for petrographical and geochemical studies as being most representative for the composition of the rhyolitic magma that produced the pyroclastic flows. All samples except Zd97-1 are affected by zeolitization, which presents a major problem for interpreting the chemical data. The emphasis here is on the petrographic observation and chemical composition of the volcanic glass in the freshest samples, melt inclusions in quartz crystals, and phenocrysts in the pumice clasts. The phenocrysts are described in order of decreasing abundance of quartz, sanidine, plagioclase, biotite, magnetite and ilmenite. Their chemical composition is shown in Tables 1 and 2.

Quartz is the most abundant phenocryst in the samples. It exhibits marginal resorbtion or embayment. Many crystals are broken, probably during the emplacement of the tuffs. Melt inclusions are often (Fig 5a).

Table 1. *Representative microprobe analyses of feldspars from the Nanovitsa depression ignimbrites*
Таблица 1. *Представителни микросондови анализи на фелдшпати от игнимбрити от Нановшката депресия*

	Zd97-1							Db10a1				Db12					
	Pl	Pl	Pl	Pl	San	San	San	Pl	Pl	Pl	San	San	San	Pl	Pl	Pl	San
	core	core	rim	rim	core	core	rim	core	core	rim	core		rim		core	rim	core
SiO_2	64.91	65.75	72.78	64.39	66.63	65.66	66.30	65.51	63.75	63.89	65.57	66.48	64.47	64.42	64.90	63.99	67.27
Al_2O_3	21.88	21.13	15.57	20.43	19.28	18.69	18.89	23.22	23.39	23.76	19.24	19.25	19.20	22.94	22.82	22.85	19.74
FeO	0.20	0.06	0.70	0.11	0.03	0.12	0.08	0.19	0.19	0.20	0.12	0.14	0.09	0.24	0.17	0.23	0.10
MnO	0.03	0.01	0.11	0.00	0.02	0.00	0.00	0.00	0.00	0.00	0.00	0.04	0.00	0.04	0.03	0.01	0.03
MgO	0.00	0.00	0.41	0.00	0.00	0.00	0.02	0.01	0.04	0.00	0.00	0.00	0.00	0.03	0.00	0.01	0.00
CaO	2.82	2.12	1.42	1.78	0.15	0.12	0.10	3.29	4.22	4.63	0.18	0.18	0.18	3.34	3.12	3.52	0.20
Na_2O	9.58	9.75	7.33	9.13	3.87	3.96	3.90	8.71	8.38	8.37	3.39	3.77	3.70	9.07	9.16	9.04	3.96
K_2O	1.01	1.18	1.3	1.87	10.78	11.18	11.11	1.50	1.17	1.07	11.73	11.17	10.55	1.36	1.39	1.13	10.80
SrO	0.03	0.05	0.00	0.00	0.00	0.08	0.02	0.04			0.00	0.04		0.05			
BaO	0.00	0.00	0.00	0.00	0.00	0.00	0.00	0.00			0.05	0.00		0.00			
Total	100.46	100.05	99.62	97.71	100.76	99.81	100.42	102.47	101.14	101.92	100.28	101.07	98.19	101.49	101.59	100.78	102.1
An	13.2	10.0	8.7	8.7	0.8	0.6	0.5	15.8	20.3	22.0	0.9	0.9	0.9	15.6	14.6	16.6	1.0
Ab	81.2	83.3	81.7	80.5	35.0	34.8	34.6	75.6	73.0	71.9	30.2	33.6	34.4	76.8	77.6	77.1	35.4
Or	5.6	6.6	9.5	10.8	64.2	64.6	64.9	8.6	6.7	6.1	68.8	65.5	64.6	7.6	7.8	6.3	63.6
Cn	0.0	0.0	0.0	0.0	0.0	0.0	0.0	0.0	0.0	0.0	0.1	0.0	0.0	0.0	0.0	0.0	0.0
Si	2.858	2.899	3.163	2.881	2.991	2.984	2.995	2.830	2.795	2.782	2.976	2.986	2.973	2.817	2.831	2.815	2.982
Al	1.136	1.098	0.798	1.077	1.020	1.001	1.006	1.182	1.209	1.219	1.029	1.019	1.044	1.182	1.173	1.185	1.031
Fe	0.007	0.002	0.025	0.004	0.001	0.005	0.003	0.007	0.007	0.007	0.005	0.005	0.003	0.009	0.006	0.008	0.004
Mn	0.001	0.000	0.004	0.000	0.001	0.000	0.000	0.000	0.000	0.000	0.000	0.002	0.000	0.001	0.001	0.000	0.001
Mg	0.000	0.000	0.027	0.000	0.000	0.000	0.001	0.001	0.003	0.000	0.000	0.000	0.000	0.002	0.000	0.001	0.000
Ca	0.133	0.100	0.066	0.085	0.007	0.006	0.005	0.152	0.198	0.216	0.009	0.009	0.009	0.156	0.146	0.166	0.009
Na	0.818	0.833	0.618	0.792	0.337	0.349	0.342	0.730	0.712	0.707	0.298	0.328	0.331	0.769	0.775	0.771	0.340
K	0.057	0.066	0.072	0.107	0.617	0.648	0.640	0.083	0.065	0.059	0.679	0.640	0.621	0.076	0.077	0.063	0.611
Ba	0.000	0.000	0.000	0.000	0.000	0.000	0.000	0.000	0.000	0.000	0.001	0.000	0.000	0.000	0.000	0.000	0.000
Sr	0.001	0.001	0.000	0.000	0.000	0.002	0.001	0.001	0.000	0.000	0.000	0.001	0.000	0.001	0.000	0.000	0.000

Table 2. *Representative microprobe analyses of biotite (Bt), magnetite (Mt) and ilmenite (Ilm) from the Nanovitsa depression ignimbrites*
Таблица 2. *Представителни микросондови анализи на биотит (Bt), магнетит (Mt) и илменит (Ilm) от игнимбрити от Нановишката депресия*

	Zd97-1	Db10a1	Db12	Db12	Db10a1	Db12	Db12	Db10a1	Db12	Db12
	Bt	Bt	Bt	Bt	Mt	Mt	Mt	Ilm	Ilm	Ilm
SiO_2	37.97	38.29	38.63	38.57	0.24	0.43	0.07	0.06	0.00	0.00
TiO_2	3.26	4.49	3.50	4.24	6.93	4.97	5.09	42.63	44.09	43.32
Al_2O_3	13.26	13.61	13.31	13.09	3.35	1.05	1.04	0.07	0.03	0.04
Cr_2O_5	0.16	0.00	0.00	0.00	0.04	0.03	0.00	0.00	0.02	0.00
FeO	15.41	16.19	15.61	15.99	76.75	80.83	81.51	52.62	50.12	48.76
MnO	1.59	0.52	0.96	0.75	0.81	2.16	2.06	2.43	4.12	3.86
MgO	13.52	14.59	15.30	15.04	1.77	0.56	0.71	1.53	1.37	1.46
CaO	0.10	0.10	0.02	0.01	0.03	0.04	0.10	0.00	0.00	0.03
Na_2O	0.36	0.42	0.32	0.52	0.00	0.03	0.00	0.05	0.00	0.08
K_2O	9.18	8.69	9.18	9.30	0.05	0.02	0.00	0.00	0.00	0.00
F	1.11	0.67	0.95	0.93						
Cl	0.10	0.09	0.11	0.11						
Total	96.02	97.66	97.89	98.55	89.97	90.13	90.58	99.39	99.83	97.54
Mg#	61.0	61.6	63.6	62.6						

Plagioclase is normally or reversely zoned albite to oligoclase (Table 1, Fig 5b). The sodic content of plagioclase is higher in the stratigraphically lowest flow of the Sapdere ignimbrite (An_{14-17}). It decreases in the upper flow of the section to An_{16-20}, with the outermost rim reaching An_{22}. This change in the plagioclases composition probably reflects either the presence of a zonal magma chamber in which the most evolved fraction was situated in the upper part of the chamber or injection of more primitive magma at the bottom of magma chamber.

Sanidine occurs in quantities approaching these of quartz. Incipient resorbtion is common, but less prominent than in quartz (Fig. 5b). The composition is relatively constant at Or_{65}.

Biotite comprises about 5% of the rocks. It occurs as euhedral or slightly corroded crystals, with the Mg content slightly increasing from the lower (Mg# 61.0) to upper flows (Mg# 63.6). Although rather small, this variation seems to confirm the suggestion of a zoned magma chamber.

Titanium-magnetite and ilmenite are rare. Ilmenite is characterized by Mn enrichment up to 4.1 wt.% in the lower Sapdere ignimbrite, which is almost twice that of the upper flow.

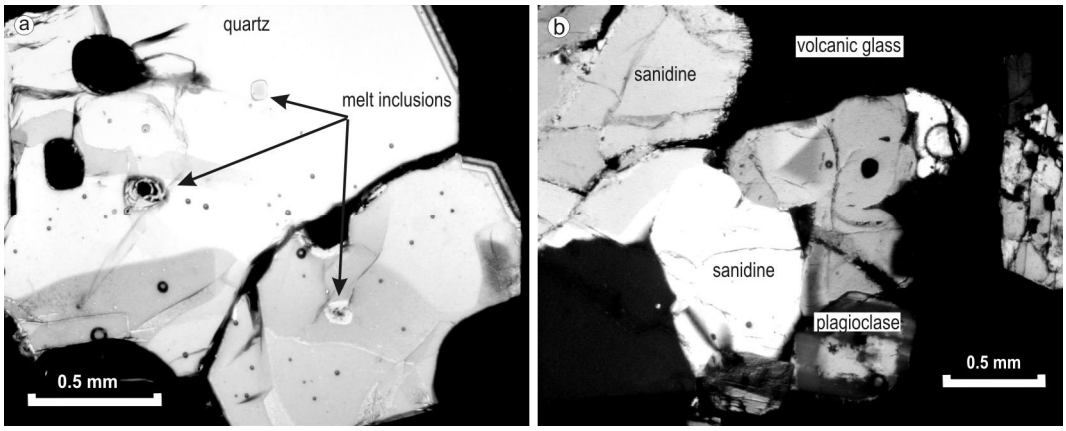

Fig. 5. Photomicrographs of pumice clasts from Sapdere ignimbrites showing: a) melt inclusions in the quartz phenocrysts and b) incipient resorbtion of sanidine and reversed zonation of plagioclase (× N)
Фиг. 5. Микроскопски снимки на пемзови късове от Сапдерески игнимбрит, показващи: а) стъклени включения в кварцов фенокристал и b) начално разтваряне на санидин и обратна зоналност в плагиоклаз (× N)

Post-depositional processes

The rocks suffered several post-depositional processes: incipient welding and compaction of the glassy shards and pumices; devitrification of the metastable volcanic glass, and vapour-phase crystallization. Individual glass shards can be identified by devitrified crystals radiating from the shard walls toward the inner part of the shard, thus forming a characteristic axiolitic texture (Ross, Smith, 1960).

Compaction and welding are evident in the deformation of glass shards and pumice fragments. The flattening of the ignimbrites is demonstrated by the collapse of Y-shaped shards and bubble walls; the alignment of elongate crystal and lithic fragments; the folding of shards around lithic and crystal fragmens; and the collapse of pumice fragments into glassy lenticular masses called fiamme. The degree of welding is variable, with most of the rocks being moderately welded. As a result of these processes, the ignimbrites were indurated and nowadays are strong and coherent rocks, more resistant to erosional processes than the underlying rhyolitic tuffs and sedimentary rocks.

The results from the X-ray diffraction analyses show that the volcanic glass of the ignimbrites is thoroughly altered to zeolitic minerals, mainly clinoptilolite and mordenite. The chemical composition of the zeolites is described by Alexiev and Djourova (1981).

Major elements

The composition of pyroclastic rocks from the Nanovitsa depression has been generally described as rhyolitic, though not a single analysis of whole rock or pumice clast has been previously published.

Chemical analyses of selected pumices and electron microprobe analyses of melt inclusions in quartz phenocrysts prove that the pyroclastic rocks have a rhyolitic composition (Table 3; Fig. 6a). The low total of the analyses is probably due to the total zeolitization of the volcanic glass. For the purpose of this study, we consider that the composition of

Table 3. *XRF and ICP-MS analyses of large pumice clasts and microprobe analyses of a perlitic groundmass and melt inclusions in quartz phenocrysts*

Таблица 3. *XRF и ICP-MS анализи на едри пемзови късове и микросондови анализи на перлитова основна маса и стъклени включения в кварцови фенокристали*

Sample N	Zd97-1	Zd97-1	Db10a1	Db10a1	Db10a2	Db10b	Db12	Db12
	pumice	perlitic groundmass	pumice	melt inclusion	pumice	pumice	pumice	melt inclusion
SiO_2	75.35	70.88	62.05	72.84	58.71	70.21	68.00	74.19
TiO_2	0.04	0.05	0.20	0.08	0.24	0.13	0.20	0.12
Al_2O_3	11.95	11.70	11.20	12.19	9.17	10.61	6.60	12.22
Fe_2O_3	0.04		0.39		0.34	0.39	0.29	
FeO	0.45	0.57		0.49				0.31
MnO	0.12	0.20	0.03	0.05	0.03	0.02	0.01	0.11
MgO	0.05	0.16	0.55	0.03	0.30	0.50	0.32	0.06
CaO	0.50	0.40	1.90	0.37	1.19	1.67	1.11	0.29
Na_2O	2.65	2.36	0.83	2.33	0.85	0.72	0.47	2.85
K_2O	5.47	6.13	3.46	5.21	4.31	3.21	2.66	4.60
P_2O_5	0.01		0.01		0.02	0.02	0.01	
LOI	3.36		6.18		3.60	5.52	3.93	
Total	99.99	93.22	86.81	93.87	78.76	93.00	83.60	94.75
Sc	4		4		3	3	2	
V	2		7		6	8	4	
Cr	bdl		8		7	9	9	
Co	bdl		2		2	2	2	
Ni	bdl		2		2	2	2	
Zn	26		21		18	18	13	
Cu	bdl		8		6	4	7	
Pb	40.8		30		81	42	38	
Ga			8		13	9	7	
Zr	61		21		54	56	30	
Hf	3.31							
Nb	27.47		14		22	32	19	
Ta	2.58							
U	12.48		2		5	54	56	
Y	37.4		1		11	2	19	
Th	23.5		21		36	48	26	
Rb	351		310		285	235	159	
Cs	13.83							
Sr	11		1583		781	676	527	
Ba	31		16		59	47	102	
La	28.43		11		38	11	15	
Ce	36.10		14		127	16	38	
Pr	4.13							
Nd	15.41		6		27	5	14	
Sm	4.63							
Eu	0.21							
Gd	4.66							
Tb	0.89							
Dy	5.78							
Ho	1.23							
Er	3.66							
Tm	0.58							
Yb	3.84							
Lu	0.61							

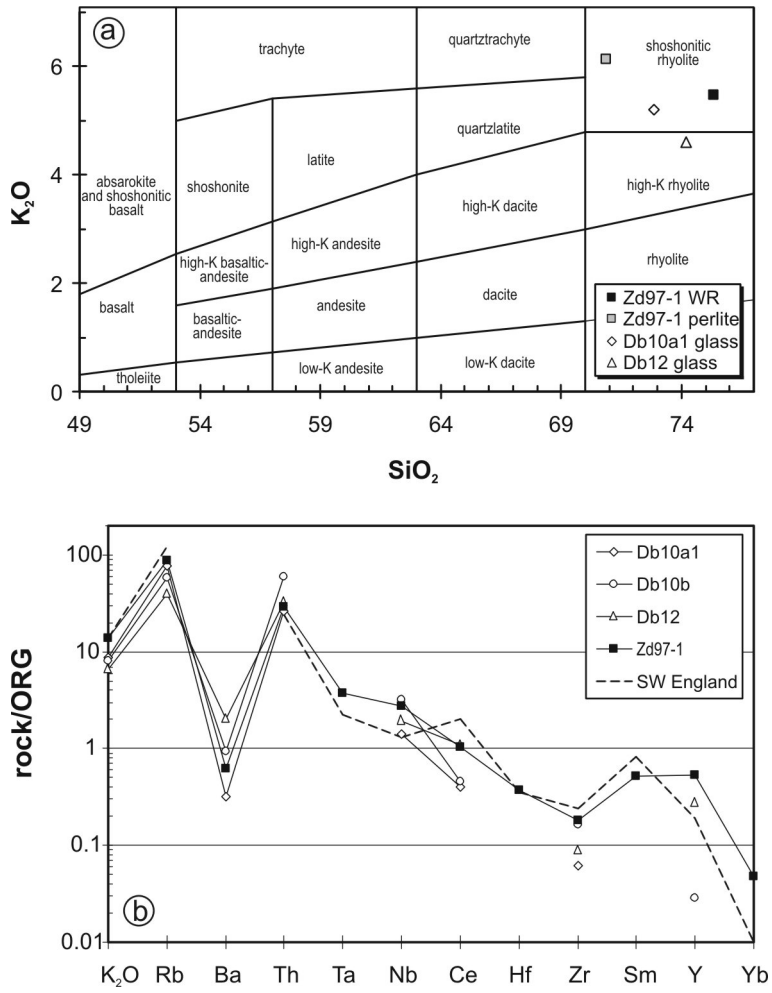

Fig. 6. a) K_2O – SiO_2 classification diagram (Peccerillo, Taylor, 1976 with modifications of Marchev, 1986); b) ORG-normalized trace elements patterns of ignimbrites from the Nanovitsa depression, Eastern Rhodopes (after Pearce et al., 1984). Samples Db10a1 and Db12 are from Sapdere ignimbrites and sample Zd97-1 is from Raven ignimbrites. The dash line represents a collisional granite from South England (after Pearce et al., 1984)

Фиг. 6. a) K_2O – SiO_2 класификационна диаграма (по Peccerillo, Taylor, 1976 с модификации на Marchev, 1986); b) Нормализирана към океанско хребетен гранит спайдер диаграма за анализи на пемзи от игнимбритите от Нановишкото понижение (по Pearce et al., 1984). За сравнение е нанесен колизионнен гранит от Южна Англия (по Pearce et al., 1984)

sample Zd97-1 and the melt inclusions in the quartz are the best approximates to the real composition of the magma. The pyroclastic rocks can be classified as high-silica and high-K rhyolites. The total of alkalis ($Na_2O + K_2O$) is about 8 wt%, with K_2O/Na_2O ratio = 2.

Trace elements

Trace elements concentrations in the analyzed samples are typical of highly fractionated rhyolitic magmas: high concentrations of incompatible elements (Rb, Th, U) and low concentrations of compatible elements (Sc, V, Cr, Co, Ni). The trace element distribution patterns (Fig. 6b) show a strong positive Rb and Th anomaly and a negative Ba anomaly. These trace-element distribution patterns are similar to most of the other rhyolitic rocks of the Eastern Rhodopes (Yanev, 1998).

Crystallization conditions

Equilibration temperature for the phenocrysts in the Nanovitsa ignimbrites was calculated from the compositions of co-existing feldspars or Fe-Ti oxides, using three different methods. Feldspar temperatures were calculated using sanidine and rim composition of plagioclase. Temperatures obtained by the methods of Stormer (1975) (643-669°C) are slightly lower than those obtained by the method of Furhman and Lindsley (1988) (660-719°C). Temperatures calculated by the titanomagnetite-ilmenite pairs (735-743°C), using the thermometer of Anderson et al. (1993), are higher compared to those obtained by the two-feldspar methods.

The estimated pressure, using the method of Stormer and Whitney (1985) is about 2-3 kbar. Oxygen fugacity was calculated with the QUILF program (Andersen et al., 1993) from the composition of two pairs of coexisting Fe-Ti oxides, which passed the magmatic equilibrium test for Mg/Mn partitioning equilibrium of Bacon and Hirshman (1988) (see Fig. 7) The results show that log fO_2 is about -13.3 for temperatures of 740°C, about two logarithmic units below the Ht-Mt buffer.

Water content can be deduced from the quartz-hosted melt inclusions in the pumice clasts. Analyses of two melt inclusions (Table

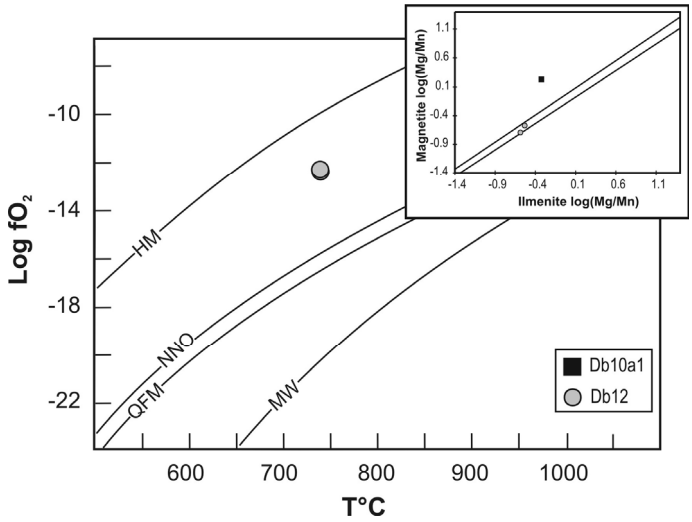

Fig. 7. *T-f*O_2 plot after Giorsho and Sack (1991), calculated from the composition of the eqiulibrium Fe-Ti oxide pairs. Inset shows the magmatic equilibrium test of Bacon and Hirshman (1988) for Fe-Ti oxide pairs from Sapdere ignimbrites. The two lines contour is the equilibrium field

Фиг. 7. *T-f*O_2 диаграма по Giorsho & Sack (1991), построена за съставите на равновесни двойки Fe-Ti оксиди. Врезката показва тестът за магматично равновесие на Bacon & Hirshman (1988) за двойки Fe-Ti оксиди от Сапдеренски игнимбрит. Двете линии очертават равновесното поле

3) show totals of 93.87-94.75, suggesting 5.25-6.13% water, which can be interpreted to represent dissolved H_2O content of the melt at the time of quenching (see Sisson and Layne, 1993). The water would be saturated at lithostatic pressures of 1.8-2.7 kbar (program of Holloway and Blank, 1994), which is very close to the pressure estimates using the method of Stormer and Whitney (1995).

Age of the pyroclastic rocks

Harkovska et al. (1992) consider the age of the pyroclastic rocks in the depression as Upper Eocene based on microfossil analyses of the marls, sandstones and limestones. This age, however, is not consistent with the stratigraphic position of the pyroclastic rocks that overlie the volcanic rocks of Zvezdel and Dambaluk volcanoes, and the precisely dated pyroclastic flows from the Borovitsa caldera (31.93±0.50 Ma, Singer and Marchev; 31.82±0.14 Ma, Moskovski et al., 2004). A high quality $^{40}Ar/^{39}Ar$ laser fusion date from sanidine in the Raven ignimbrites yielded an age of 31.13 ±0.12 Ma (Table 4), confirming the observed stratigraphic relations of pyroclastic rocks in Nanovitsa depression.

Discussion

Assessment for the source of the Nanovitsa pyroclastic rocks

One of most intriguing questions for the Nanovitsa Depression pyroclastic rocks is the location of the vent(s). The eruption of these quite extensive ignimbrite sheets and air-fall tuff was possibly associated with a caldera collapse. However, so far, such a structure has not been identified, although some authors (e.g. Georgiev et al., 2000) on the basis of negative gravity anomalies suggest that the Nanovitsa depression itself is a caldera structure. The absence of any magmatic activity in the depression is the strongest evidence against such a statement. The large blocks of rhyolites mixed with blocks of andesites that have been described by Harkovska and Djurova (1994) in a slump southeast of Dambaluk are the only evidence of some magmatic activity close to the depression. However, our observation of these blocks suggests that they are strongly welded and silicified ignimbrites rather than rhyolites.

Table 4. *Individual* $^{40}Ar/^{39}Ar$ *laser-fusion analyses of 6 sanidine grains from a pumice clast from the Raven pyroclastic flow (sample Zd 97-1)*
Таблица 4. *Индивидуални* $^{40}Ar/^{39}Ar$ *анализи на 6 санидинови кристала от пемзов къс от Равенските игнимбрити (образец Zd 97-1)*

Sample	Experiment number	$^{40}Ar/^{39}Ar$	$^{37}Ar/^{39}Ar$	$^{36}Ar/^{39}Ar$	$^{40}Ar^{*}$ (10^{-14} mol)	% $^{40}Ar^{*}$	K/Ca	Apparent age ± 2σ Ma		
Zd97-1										
Sanidine	GE117X4A	1.363	0.00562	0.0000280	0.88	99.1	87.14	31.19	±	0.16
J=0.01291	GE117X4B	1.462	0.00581	0.0003688	0.79	82.3	84.34	31.14	±	0.20
±0.13%	GE117X4C	1.430	0.00607	0.0002573	0.56	94.3	80.69	31.17	±	0.20
	GE117X4D	1.434	0.14477	0.0003161	0.37	94.0	3.38	31.12	±	0.24
	GE117X4E	1.390	0.05004	0.0001362	0.78	97.1	9.79	31.15	±	0.16
	GE117X4F	1.418	0.06225	0.0002601	0.40	94.6	7.87	30.97	±	0.22
						mean & SD		31.12	±	0.18
						weighted mean & SD		31.13	±	0.12

The Borovitsa caldera is another possible source for the Nanovitsa ignimbrites. It is the largest caldera recognized in the Eastern Rhodopes (Ivanov, 1972) located just 20 km from the western edge of the depression. However, the latest magmatic activity at Borovitsa, dated at 31.75 ± 0.34 Ma (Singer, Marchev, 2000) is older than the age of Nanovitsa ignimbrites (31.13 ± 0.12 Ma). Moreover, late Borovitsa rhyolites are amphibole-bearing (Marchev, Fekeldjiev, 1980), whereas Nanovitsa ignimbrites are amphibole-free. In addition, careful examination of the orientation of the branches of the petrified forest, as discussed above, implies that the vent(s) were located to the northeast. Unfortunately, no caldera or even acid rocks of similar age are identified in the Sveti Ilia volcano, which is located in that direction.

Conclusions

Oligocene (~31 Ma) pyroclastic rocks, outcropping in the Nanovitsa depression, seem to represent the final stages of volcanic activity in the Eastern Rhodopes. Field observations show that the beginning of the pyroclastic activity occurred in a shallow marine environment, which formed the Raven ignimbrites. Following this, a sequence of air-fall tuffs and pyroclastic flows was deposited in a sub-aereal environment, as shown by the buried forest in the canyon of the Sapdere river.

The petrified forest is an impressive natural phenomenon and provides an opportunity for detailed volcanological studies and environmental education.

The pyroclastic rocks are of rhyolitic composition with mineral composition variations showing indications that the felsic magma was zoned and, probably, underlain by a more mafic magma. The crystallization of the rhyolitic magma took place at 5-10 km depth, temperatures of 740-650°C, high volatile content (5-6 wt.%), and high oxygen fugacity.

A major unresolved question is the location of the source of pyroclastic activity. Eruptions of this magnitude would have produced a caldera structure, but such a structure is not known in the close vicinity. Further field and precise age studies are needed in order to solve the problem.

Acknowledgments: We would like to thank B. Singer for his cooperation in running sanidine from sample Zd97-1 for $^{40}Ar/^{39}Ar$ age determination; O. Vaselli for help with microprobe facilities and XRF analyses at the Centro di studi per la Minerogenesi e Geochimica Applicata, University of Florence. We thank Raya Raycheva for her assistance in the field and valuable suggestions and Kevan Aswort for his assistance in improving the English. Constructive criticism by Yotzo Yanev led to a much-improved manuscript. Funding for this work was provided by the Swiss National Science Foundation (project 7BUPJ02276).

References

Alexiev, B., E. Djourova. 1981. Characteristic and estimation of the zeolitic rocks south of river Arda, between the rivers Varbitsa and Krumovitsa. *Geofond NIS –SU*; 153 p. (in Bulgarian).

Anderson, D., D. Lindsley, P. Davidson. 1993. QUILF: a PASCAL program to assess equilibria among Fe-Mg-Mn-Ti oxides, pyroxenes, olivine and quartz. *Computers and Geosciences,* **19**, 1333-1350.

Bacon, C., M. Hirshmann. 1988. Mg/Mn partitioning as a test for equilibrium between coexisting Fe-Ti oxides. *Amer. Mineral.,* **73***, 57-61.*

Bahneva, D., N. Stefanov. 1974. Paleovolcanologic characterization of the trachyrhyolitic volcanism south of "Studen Kladenets" dam, Kardzhali district. *Annual of MGU, part. II-geol.*, **20**, 7-32 (in Bulgarian).

Bence, A., A. Albee. 1968. Empirical correction factors for the electron microanalysis of silicate and oxides. *Journ. Geol.*, **76**, 382-403.

Boyanov, I., A. Goranov. 2001. Late Alpine (Paleogene) superimposed depressions in parts of Southeast Bulgaria. *Geol. Balcanica*, **31** (3-4), 3-36.

Cas, R., J. Wright. 1988. *Volcanic successions; Modern and ancient.* London, Chapman & Hall, 528 p.

Creber, G., S. Ash. 2004. The late Triassic Schilderia adamanica and Woodworthia arizonica trees of the Petrified Forest National Park, Arizona, USA. *Palaeontology*, **47**, 21-38

Duffield, W., G. Dalrymple. 1990. The Taylor Creek Rhyolite of New Mexico: a rapidly emplaced field of lava domes and flows. *Bull. Volcanol.,* **52**, 475-487.

Fisher, R.V., 1961. Proposed classification of volcaniclastic sediments and rocks. *Geol. Soc. Am. Bull.,* **72**, 1409-1414.

Francis, P., 1993. *Volcanoes. A Planetary Perspective.* Oxford University Press, New York. 443 p.

Furhman, M., P. Lindsley. 1988. Ternary feldspar modelling and thermometry. *Amer. Mineral.,* **73**, 201-215.

Georgiev, V., L. Nikova, P. Milovanov. 2000. Paleovolcanoes in part of the Eastern Rhodopes. *ABCD-GEODE 2000 Workshop, Abstracts.*

Ghiorso, M., R. Sack. 1991. Fe-Ti oxide geothermometry: Thermodynamic formulation and the estimation of intensive variables in silicic magmas. *Contrib. Mineral. Petrol.*, **108**, 485-510.

Goranov, A. 1960. Lithology of the Paleogene deposits in parts of the Eastern Rhodopes. *Trav. Géol. Bulgarie, Sér. Géochimie, Gîtes métallifères et non-métallifères*, **1**, 258-310 (in Bulgarian).

Goranov, A., D. Kozhoukharov, I. Boyanov, E. Kozhoukharova, 1995. *Geological Map of Bulgaria, Scale 1:100 000. Sheet Kroumovgrad and Sape.* Sofia.

Harkovska, A. 1992. Petrified forest in Momchilgrad region. *Nauka i Znanie,* **2/3**, 46-48 (in Bulgarian).

Harkovska, A., S. Moskovski, S. Juranov. 1992. Upper Eocene (Priabonian) rhyolite tuffs in the region of Dambaluk Mountain (East Rhodopes, Bulgaria). *Geol. Balcanica,* **22**, (1), 74.

Harkovska, A., E. Djourova. 1994. Petrologic features and slump redeposition of Paleogene rhyolitic tuffs from Eastern Rhodopes (Bulgaria). *Int. Volcanol. Congr. IAVCEI 1994*, Ankara, Abstracts.

Holloway, J., J. Blank. 1994. Application of experimental results to C-O-H species in natural melts. In: M.R. Carol, Holloway, J.R. (Eds.) *Volatiles in Magmas*. Mineral. Soc. America, Rev. Mineral., **30**, 187-230.

Ivanov, R. 1960. Magmatism in Eastern Rhodope Paleogene depression. Pt. 1 - Geology. *Trav. Géol. Bulgarie, Sér. Géochimie, Gîtes métallifères et non-métallifère,* 1, 311-387 (in Bulgarian).

Ivanov, R. 1961. Upon the geology of Dambalak volcanic massif, Momchilgrad area. *C. R. Acad. bulg. Sci.*, 9, 143-151 (in Bulgarian).

Ivanov, R. 1972. Volcano-tectonic structures in the Borovitza depression. *Bull Geol. Inst., Ser. Geochem. Mineral. Petrogr.* **21**, 193-210.

Marchev, P., G. Fekeldgiev. 1980. A petrographic characteristic of the fineporphyritic potassium and ultrapotassium rhyolites from the deposits of the village Bezvodno and the possibility of their application in the fine ceramic industry. *Ann. Univer. Sofia, Fac. Geol., Geogr.* **72**, 1-geology, 157-168 (in Bulgarian with English abstract).

Marchev, P. 1986. Extension of the subdivision and nomenclature of the shoshonitic rocks. *C. R. Acad. bulg. Sci*, 39, 69-71 (in Russian).

Marchev, P., G. Rogers, R. Conrey, J. Quick, O. Vaselli. R. Raicheva. 1998. Paleogene orogenic and alkaline basic magmas in the Rhodope zone: relationships, nature of magma sources, and role of crustal contamination. In: G. Christofides, P. Marchev, G. Serri, (Eds.), *Tertiary Magmatism of the Rhodopian Region. Acta Vulcanol.* **10**, (2), 217-232.

Marchev, P., B. Singer. 2002. $^{40}Ar/^{39}Ar$ geochronology of magmatism and hydrothermal activity of the Madjarovo base-precious metal ore district, eastern Rhodopes, Bulgaria. In: D. Blundell, F. Neubauer, A. von Quadt, (Eds.), The timing and location of major ore deposits in an evolving orogen. *Geological Society, London, Special Publications,* **204**, 137-150.

Moskovski, S., A. Harkovska, P. Marchev. 1990. Stratigraphic, petrologic and structural-volcanologic investigations in the area of Dambalak volcanic massif. *Geofond NIS –SU;* 147 p. (in Bulgarian).

Moskovski, S., V. Karloukovski, Z. Milakovska, A. Harkovska, M. Pringle. 2004. Lithological and magnetostratigraphic correlation of paleogene sections in the Eastern Rhodopes (SE Bulgaria). *Geol. Carpathica*, **55** (3), 251-260.

Pearce, J., N. Harris, A. Tindle. 1984. Trace element discrimination diagrams for the tectonic interpretation of granitic rocks. *J. Petrol.,* **25**, 956-983.

Peccerillo, A., S. R. Taylor. 1976. Geochemistry of Eocene calc-alkaline volcanic rocks from the Kastamonu area, northern Turkey. *Contrib. Mineral. Petrol.,* **58**, 63-81.

Ross, G., R. Smith. 1960. Ash flow tuffs: their origin, geologic relations and identification. *US Geol. Surv. Prof. Pap.*, **366**, 1-81.

Singer, B., P. Marchev. 2000. Temporal evolution of arc magmatism and hydrothermal activity, including epithermal gold veins, Borovitsa

caldera, southern Bulgaria. *Econ. Geol*. **95**, 1155-1164.

Sisson, T., G. Layne. 1993. H_2O in basalt and basaltic andesite glass inclusions from four subduction-related volcanoes. *Earth Planet. Sci. Lett.*, **117**, 619-635.

Stormer, J. 1975. A practical two-feldspar geothermomether. *Amer. Mineral.*, **60**, 667-674.

Stormer, J., J. Whitney. 1985. Two-feldspar and iron-titanium oxide equilibria in silicic magmas and the depth of origin of large volume ash-flow tuffs. *Amer. Mineral*. **70**, 52-64.

Yanev, Y., 1998. Petrology of the Eastern Rhodope acid volcanism. In: G. Christofides, P. Marchev, G. Serri (Eds.), *Tertiary Magmatism of the Rhodopian Region. Acta Vulcanol*. **10** (2), 265-277.

Yanev, Y., F. Innocenti, P. Manetti, G. Serri. 1998. Upper-Eocene-Oligocene collision-related volcanism in Eastern Rhodopes (Bulgaria)-Western Thrace (Greece): Petrogenetic affinity and geodynamic significance. In: G. Christofides, P. Marchev, G. Serri, (Eds.), *Tertiary Magmatism of the Rhodopian Region. Acta Vulcanol.* **10** (2), 279-291.

Accepted December 28, 2004
Приета на 28.12.2004